Sam-Yellowe's Trichrome Staining Identifies Life Cycle Stages of Free-Living Colpodellids

Tobili Y Sam-Yellowe*

Mahdi I Salti

Oluwapemi E Adeloye

Department of Biological, Geological and Environmental Sciences, Cleveland State University, Cleveland, Ohio, USA

Abstract

The colpodellids consist of free-living predatory protists phylogenetically related to pathogenic Apicomplexan parasites such as *Plasmodium* species, *Cryptosporidium* sp. and *Toxoplasma gondii*. Among the colpodellids, *Colpodella* species prey on bodonids, algae, and ciliates. *Voromonas pontica* preys on *Percolomonas* species. In the past decade, *Colpodella* species have been reported to cause opportunistic infections in humans and animals, and having the potential for zoonotic infections in humans due to the presence of *Colpodella* species in ticks. In the reported cases, transmission and pathogenic stages of *Colpodella* were not identified by light microscopy. In the colpodellid *V. pontica*, cyst stages of both the predator and its prey *Percolomonas cosmopolitus* have not been identified by light microscopy. In this study we evaluated the dye components used for Sam-Yellowe's trichrome staining, from different major vendors to determine the consistency and reproducibility of the staining protocol to aid the use of the staining protocol for diagnosis. We show that although slight variations in the color of the stained cells are obtained, life cycle stages of *Colpodella* sp. ATCC 50594 could be clearly identified, regardless of the vendor used. For the first time, Sam-Yellowe's trichrome staining series, could identify cysts of *V. pontica* and its prey, demonstrating that the staining protocol can identify life cycle stages of other colpodellids. Sam-Yellowe's trichrome staining will aid molecular diagnosis of infections caused by colpodellids in human and animals, identify colpodellids in ticks and flies and from environmental samples, when used for staining.

Keywords: Apicomplexa, *Colpodella* species, Colpodellids; *Colpodella* sp. ATCC 50594, Life cycle, Myzocytosis, Sam-Yellowe's trichrome stains, *Voromonas* cysts, *Voromonas pontica*.

Introduction

Colpodellids are free-living protists related phylogenetically to the pathogenic apicomplexans such as *Toxoplasma gondii*, *Plasmodium* sp., *Babesia* sp., and *Cryptosporidium* sp. [1]. The colpodellids which include *Colpodella* species, *Voromonas pontica* (previously *Colpodella pontica*) and *Alphamonas* are biflagellated and possess trophozoite and cyst stages in their life cycles [2]. Colpodellids prey on bodonids, ciliates and algae using the process of myzocytosis where cytoplasmic contents of the prey are aspirated into the cytoplasm of the predator. Ectoparasitic

colpodellids such as *Colpodella gonderi* and *C. tetrahymenae* attach to ciliates for prolonged feeding in contrast to the predatory attacks observed with bodonid or algal prey [3, 4]. In cyst forming species, the food vacuole associated with remnants of the cytoplasm including the nucleus, differentiates into a cyst [5-8]. Some cyst forming species also divide by longitudinal fission [7]. *Colpodella unguis* and *C. edax* do not form cysts [7,9]. *Colpodella* species have been identified in three human infections and in animal infections suggesting that these free-living protists are opportunistic pathogens and capable of infecting human and animal hosts [10-12]. A case of anemia in a relapsing infection caused by *Colpodella* sp. strain HEP, was identified using primers targeting the 18S rRNA gene of *Babesia* sp. The DNA sequence of the amplicon with homology to *C. tetrahymenae* was described in the patient from Yunan Province, Southwestern China in an erythrocyte infection similar to babesiosis [10]. A second human case reported from Heilonjiang Province, Northeast China, was tick-borne, with the patient exhibiting neurological symptoms [11]. Polymerase chain reaction (PCR) of cerebrospinal fluid using primers targeting the18S rRNA gene from *Babesia* sp. identified DNA with sequence homology to *Colpodella* species and is designated *Colpodella* spp. HLJ. The primers also identified DNA with sequence homology to *Colpodella* sp. in *Ixodes persuclatus* ticks in woodlands around the patient's living area [11]. Life cycle stages causing infection were not described, stages in the ticks were also not described and no staining was performed to identify life cycle stages of *Colpodella* spp. HLJ [10,11]. *Colpodella gonderi* was identified in the urine of a human case of urinary tract infection with an uncertain etiology, using Giemsa staining [12]. *Colpodella* species have been reported in various animals including in cattle and *Rhipicephalus microplus* ticks infesting cattle with 100% sequence identity to *Colpodella* 18S rRNA gene sequences identified from a raccoon dog in Poland [13]. *Colpodella* sp. have also been identified in raccoons, cat, dog, goats and attached *Haemaphysali longicornis* ticks, and horses [14-18]. *Colpodella* species DNA sequences identified in the blood of a South China Tiger that died of babesiosis-like symptoms after a tick bite had 90.1% sequence identity to *Colpodella* sp. strain HEP and 90.4 % sequence identity to *Colpodella* sp. strain HLJ [19]. Ticks within the tiger enclosure and grass around the enclosure also contained *Colpodella* species [19]. Oligonucleotide primers targeting18S rRNA from *Cryptosporidium* species identified *Colpodella* species from fecal samples of zoo felines in North East China [20]. For the human and animal cases reported, polymerase chain reaction (PCR) was used to identify *Colpodella* sp. DNA. However microscopic identify of life cycle stage morphology of *Colpodella* species in the human and animal hosts, ticks and flies were not described [21,22]. In two of the human cases, Giemsa staining was used to identify protists in blood and urine [10,12]. However, these were not identified as transmission or pathogenic stages and life cycle stages in erythrocytes were not easily distinguished [10]. In previous studies, we described the life cycle of *Colpodella* sp. ATCC 50594, investigated the process of myzocytosis and identified previously undocumented life cycle stages using Sam-Yellowe's trichrome staining protocols [23]. We

developed Sam-Yellowe's trichrome staining to identify and distinguish cyst stages of *Colpodella* sp. ATCC 50594 and its prey *Parabodo caudatus*. Both protists are biflagellated and form cysts of similar size, indistinguishable by Giemsa staining [24]. We identified the trophozoites of *V. pontica* and *P. cosmopolitus* in earlier studies using Giemsa staining, but were unable to differentiate the cyst stages [25]. In this study, our first goal was to evaluate the consistency and reproducibility of the dyes used for Sam-Yellowe's trichrome staining. The dyes neutral red, brilliant green and methylene blue were obtained from different major vendors, with a focus on identifying young trophozoites and cysts of *Colpodella* sp. ATCC 50594 since these stages can be obscured by bacteria or other debris in samples and in cultures. In previous staining studies, we obtained the dyes neutral red, brilliant green and methylene blue from the same vendors [24]. The vendor supplying neutral red closed operations resulting in the purchase of neutral red from a different vendor. Initial use of neutral red from the new vendor resulted in variations in the final colors on stained cells. To ensure consistency and reproducibility of the staining protocol, we also evaluated methylene blue and brilliant green from different vendors. Our second goal was to identify cyst stages of *V. pontica* and *P. cosmopolitus* using Sam-Yellowe's trichrome staining series.

Materials and Methods

Voromonas pontica Cavalier-Smith (ATCC 50640) and *Colpodella* sp. (ATCC 50594) (American Type Culture Collection, Manassas, Virginia, USA) were maintained in diprotist cultures with prey species; *Percolomonas cosmopolitus* and *Parabodo caudatus*, respectively, as described previously [25]. *Enterobacter aerogenes* bacterized Hay medium (Ward's Science, Rochester, New York, USA) was used for culture. *Voromonas pontica* was cultured in Hay medium (Ward's Science) mixed with Carolina Seawater (Carolina Biological Supply Company, Burlington, North Carolina, USA). Diprotist cultures in 25 cm^2 tissue culture flasks capped tightly with plug-seal caps were incubated at 22-24ºC. *Colpodella* sp. was cultured as described previously [25]. Cultures were examined using an inverted microscope with phase contrast and Sam-Yellowe's trichrome staining was performed to monitor cell growth. All cultures were maintained aseptically without antibiotics or filtration for bacteria elimination. *Plasmodium falciparum* (strain FCR3) was cultured as described previously and ring-infected erythrocytes fixed in absolute methanol for staining [25]. *Cryptosporidium parvum* oocysts were obtained from AlphaTec (https://www.alphatecsystems.com/).

Staining and Light Microscopy

Voromonas pontica ATCC 50640 and *Colpodella* sp. ATCC 50594 cultures were processed for formalin fixation and staining as described previously [24,25]. Smears were prepared on glass slides from the cell suspension, air-dried and either stained with Giemsa stain or Sam-Yellowe's trichrome stain. Briefly, an equal volume of 10% formalin was added to the cell cultures of *Colpodella* sp. or cell suspensions of *V. pontica* following centrifugation of culture and resuspension of the pellet in 1X PBS. Fixed cells were

centrifuged, formalin supernatants were discarded and pellets washed in 1X PBS. The formalin fixed cells were resuspended in 80 μl 1X PBS and smears prepared on glass slides for Giemsa and Sam-Yellowe's trichrome staining.

Sam-Yellowe's trichrome stain A with 0.3 % Methylene blue, 1 min; 1% Brilliant green, 5 min and 1% Neutral Red (Electron Microscopy Sciences, EMS), 1 min, Sam-Yellowe's trichrome D with 1 % crystal violet, 30 seconds; 1 % Brilliant green, 2 minutes; 1% Neutral red, 1 minute and Sam-Yellowe's trichrome I with 1 % crystal violet, 1 min; 1% Brilliant green, 2 min and 1 % Safranin, 2 min and Sam-Yellowe's trichrome K with 0.3 % Methylene blue, 1 min; 1% Fast green (aqueous), 5 min and 1% Neutral Red. Dyes from different vendors were used for Sam-Yellowe's trichrome stain A (Table 1) [24,25].

Neutral red, brilliant green and methylene blue purchased from different vendors were used in the staining protocol to evaluate differences in the final color of stained cells following staining (Table 2). The original neutral red dye obtained from ScholAR Chemistry can no longer be obtained due to the closing of the company. We therefore tested neutral red from other vendors (Tables 1 and 2). Two lots of neutral red from Ward's Science were tested, an old (O) lot of the dye and a newer (N) recently purchased lot. All stained smears were examined under oil immersion at x1000 magnification and images were captured using an Olympus BX43 compound microscope attached to an Infinity HD Lumenera digital camera and Olympus U-TV0.35xc-2 adapter using Infinity HD Capture software. Images were adjusted to 300 dpi using the CMYK color mode on Adobe photo shop (CS6).

Results

Trophozoite and cyst stages of *Colpodella* sp. ATCC 50594 were detected among the background of bacteria in the diprotist culture. Young cysts of *Colpodella* sp. were detected (Figure 1A, black arrows) and could be distinguished from mature cysts (Figure 1B, white arrows). Groups of *P. caudatus* cysts were also detected (red arrows, Figure 1B and 1C). The yellow arrows identify juvenile trophozoite stages of *Colpodella* sp. ATCC 50594 (Figure 1C). Trophozoites of *Colpodella* sp. ATCC 50594 (yellow arrow) attached to prey *P. caudatus* (red arrow) in myzocytosis were also detected among the *Colpodella* sp. ATCC 50594 cysts (Figure 2A).

Young trophozoites of *Colpodella* sp. unobscured by bacteria were detected with the flagella visible (Figure 2B and C, thick black arrows). *Voromonas pontica* stained using 1% methylene blue (Figure 3A-C) was distinguished from its prey *P. cosmopolitus* (Figure 3D) based on the number of flagella; two for *V. pontica* and four for its prey. *Voromonas pontica* (yellow arrow) attached to *P. cosmopolitus* (red arrow) in myzocytosis (Figure 3E) can also be identified showing the tubular tether (black arrow) between predator and prey.

However, similar to previous studies with *Colpodella* sp. ATCC 50594 using Giemsa staining, trophozoites of *V. pontica* could be distinguished from those of *P. cosmopolitus* but cysts could not be distinguished since both cysts stained uniformly blue. We therefore performed Sam-Yellowe's trichrome staining on formalin-fixed *V. pontica* (formerly *Colpodella pontica*) from a diprotist culture containing the prey protist *P. cosmopolitus* using Sam-Yellowe's trichrome I, shown in Figure 4.

Trophozoite stages of *V. pontica* and *P. cosmopolitus* were detected and could be distinguished by the number of flagella identified on each protist. *Percolomonas cosmopolitus* are tetraflagellate with three short flagella and a fourth long flagellum (Figure 4, black box), *V. pontica* are biflagellate with heterodynamic flagella (Figure 4, red box). *Voromonas pontica* (yellow arrow) and *P. cosmopolitus* (red arrow) attached in myzocytosis were also identified (Figure 4, green box). *Voromonas pontica* uses the process of myzocytosis to aspirate the cytoplasmic contents of the prey through the tubular tether. Using Sam-Yellowe's trichrome staining, cysts of *V. pontica* were identified for the first time as shown

1 Minute	5 Minutes	1 Minute
Fisher Chemical 0.3% Methylene Blue	ACROS 1% Brilliant Green	EMS 1% Neutral Red
EMD 0.3% Methylene Blue	ACROS 1% Brilliant Green	EMS 1% Neutral Red
EMD 0.3% Methylene Blue	ACROS 1% Brilliant Green	Ward's Science 1% Neutral Red
EMD 0.3% Methylene Blue	ACROS 1% Brilliant Green	Ward's Science 1% Neutral Red
EMD 0.3% Methylene Blue	ACROS 1% Brilliant Green	ScholAR Chemistry 1% Neutral Red
EMD 0.3% Methylene Blue	ACROS 1% Brilliant Green	Carolina 1% Neutral Red
EMD 0.3% Methylene Blue	Thermo Scientific 1% Brilliant Green	EMS 1% Neutral Red
EMD 0.3% Methylene Blue	Thermo Scientific 1% Brilliant Green	ScholAR Chemistry 1% Neutral Red
EMD 0.3% Methylene Blue	Hardy Diagnostic 1% Brilliant Green	EMS 1% Neutral Red
EMD 0.3% Methylene Blue	Hardy Diagnostic 1% Brilliant Green	SchoAR Chemistry 1% Neutral Red
EMD 0.3% Methylene Blue	Sigma 1% Fast Green	EMS 1% Neutral Red
EMD 0.3% Methylene Blue	Sigma 1% Fast Green	ScholAR Chemistry 1% Neutral Red
EMD 0.3% Methylene Blue	Carolina 1% Methyl Green	EMS 1% Neutral Red
EMD 0.3% Methylene Blue	Carolina 1% Methyl Green	ScholAR Chemistry 1% Neutral Red
EMD 0.3% Methylene Blue	Ward's Science 1% Malachite Green	EMS 1% Neutral Red
EMD 0.3% Methylene Blue	Ward's Science 1% Janus Green	EMS 1% Neutral Red
EMD 0.3% Methylene Blue	Ward's Science 1% Janus Green	ScholAR Chemistry 1% Neutral Red
EMD 0.3% Methylene Blue	Carolina 0.5% Fast Green Alcohol	EMS 1% Neutral Red
EMD 0.3% Methylene Blue	Carolina 0.5% Fast Green Alcohol	ScholAR Chemistry 1% Neutral Red

Table 1: Sam-Yellowe's trichrome staining protocol with dyes from different vendors.

| Dye	Vendor	Website Link
Neutral Red	Electron Microscopy Sciences	https://www.emsdiasum.com/
	Ward's Natural Science	https://www.wardsci.com/store/
	Carolina	https://www.carolina.com/
	ScholAR Chemistry	Company closed
Brilliant Green	Hardy Diagnostics	https://hardydiagnostics.com/
	Thermo Scientific	https://www.thermofisher.com/us/en/home.html
	ACROS/ Thermo Scientific	
Methylene Blue	Harleco EMD	https://www.emdmillipore.com/US/en/product/Methylene-Blue-Chloride
	Fisher Chemical	https://www.fishersci.com/us/en/brands/I8T3NQD9/fisherchemical.html
Janus Green	Ward's Science	https://www.wardsci.com/store/
Malachite Green	Ward's Science	https://www.wardsci.com/store/
Fast Green 0.5% Alcohol	Carolina	https://www.carolina.com/
Methyl Green	Carolina	https://www.carolina.com/
Fast Green FCF	Sigma	https://www.sigmaaldrich.com/US/en

Table 2: Dyes from Major Vendors.
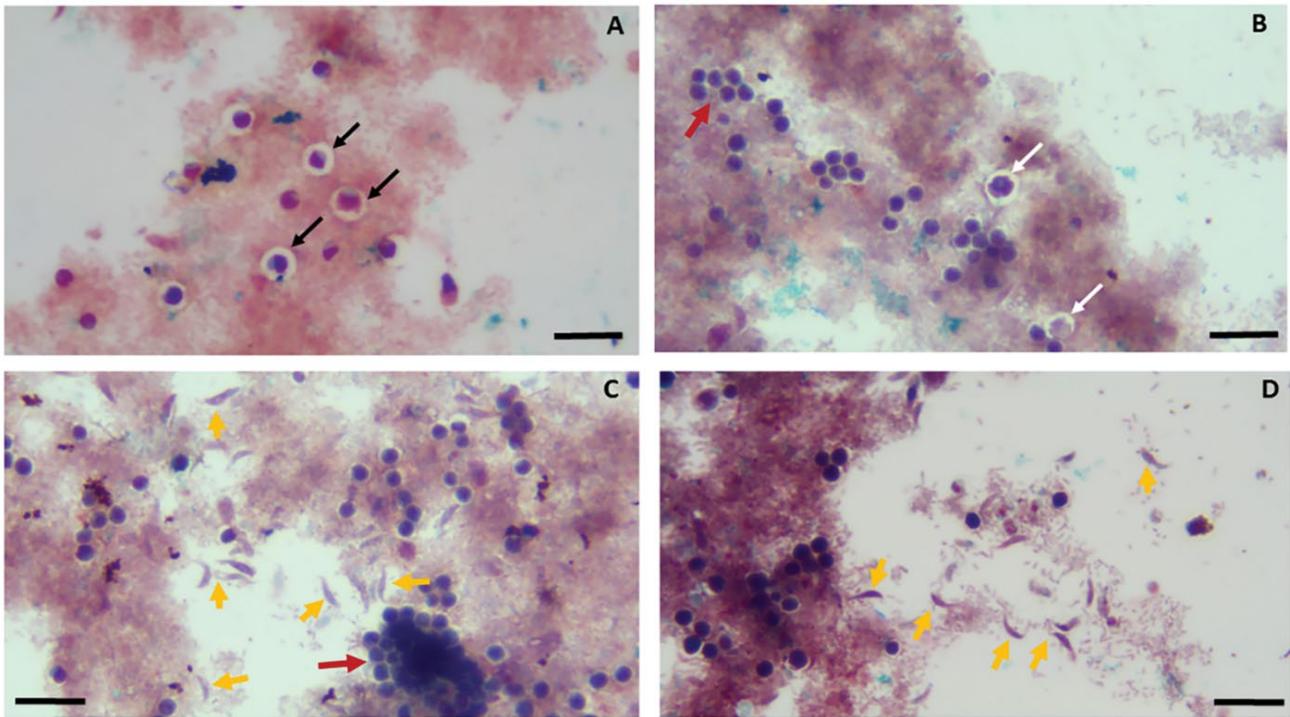
Figure 1: Sam-Yellowe's trichrome A staining of the predator *Colpodella* sp. ATCC 50594 cysts and young trophozoite stages (yellow arrows). A. Young dual-colored demilune cysts of *Colpodella* sp. ATCC 50594 showing a partially light blue-white and dark blue-purple staining pattern (black arrows). B. Mature *Colpodella* sp. ATCC 50594 cysts are shown in panel B (white arrows) showing the initiation of division with the appearance of two to three "lobes" with an even dark blue-brownish appearance. Young fusiform-shaped trophozoites of *Colpodella* sp. ATCC 50594 are shown in panels C and D (yellow arrows). Clusters of *Parabodo caudatus* (prey) cysts are indicated by the red arrows (panels B and C). Background of cells shown are bacteria from the diprotist culture. Anti-bacterial zones were observed around the young and mature cysts of *Colpodella* sp. 50594 (black and white arrows). Two different lots of neutral red purchased at different times from ScholAR Chemistry were used for staining. 1% neutral red used in panel A was an older lot. In panels B-D a second dye lot from ScholAR Chemistry was used before the company closed. Cells from diprotist culture were formalin-fixed. Scale bars, 20 μm.

in figure 5A-D (black arrows). *Voromonas pontica* cysts bear morphological resemblance to the young demilune cysts of *Colpodella* sp. ATCC 50594, with the partially white-blue-purple color described for *Colpodella* cysts. The cysts of *V. pontica* were identified and found mostly in clusters. Evenly stained, round cysts identified in the culture are cysts of *P. cosmopolitus* (white arrow).

In order to determine if Sam-Yellowe's trichrome staining series could stain and distinguish life cycle stages of pathogenic apicompexans, blood stages of methanol-fixed *P. falciparum* were stained with Sam-Yellowe's trichrome A. Ring-infected (black arrows) and uninfected erythrocytes were detected (Figure 6A). Additionally, formalin-fixed *Cryptosporidium parvum* oocysts were also stained with Sam-
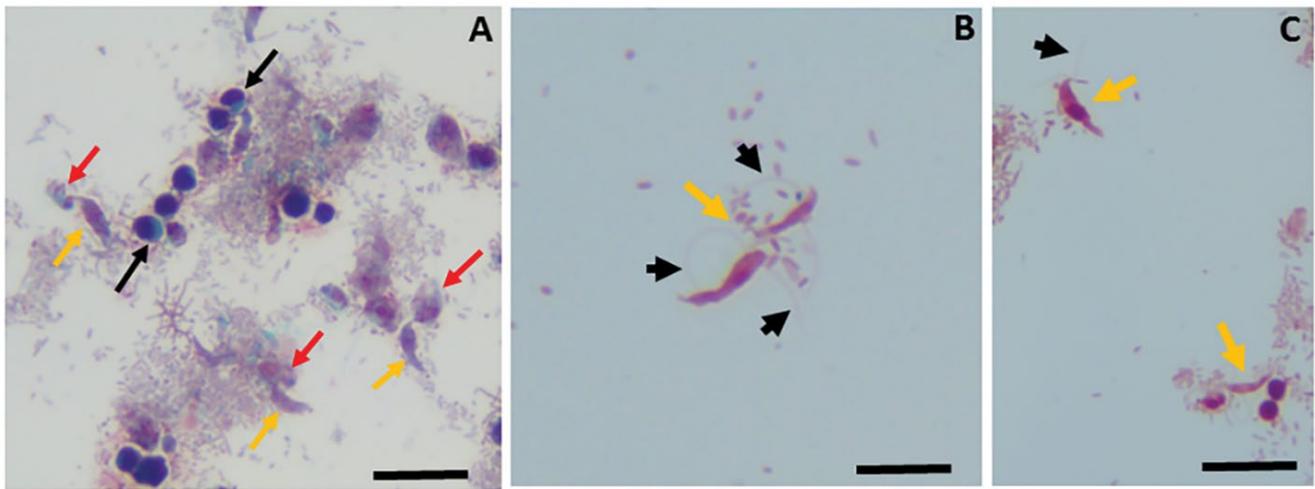
Figure 2: *Colpodella* sp. ATCC 50594 cysts, trophozoites, young trophozoite stages (yellow arrows) and predator and prey in myzocytosis stained with Sam-Yellowe's trichrome A staining protocol. Panel A shows young *Colpodella* sp. ATCC 50594 cysts (black arrows) staining partially light blue-white and dark blue-purple, and the predator *Colpodella* sp. ATCC 50594 (yellow arrows) and the prey *P. caudatus* (red arrows) attached in myzocytosis. Panels B and C show young trophozoites of *Colpodella* sp. 50594 with flagella indicated by thick black arrows. One % neutral red purchased from EMS was used in panels A-C. Cells from diprotist culture were formalin-fixed. Scale bars, 20 μm.
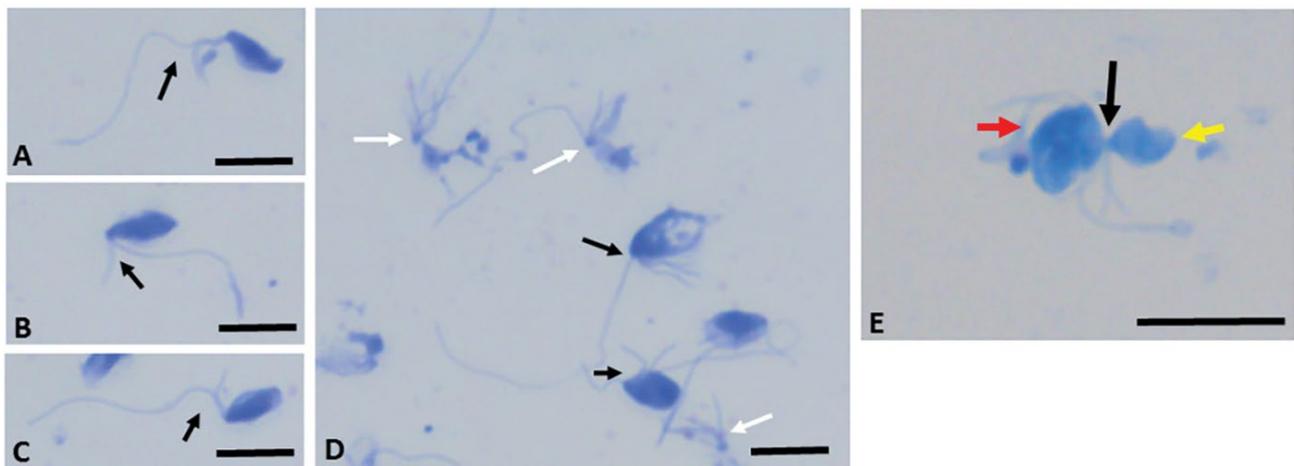
Figure 3: 1% Methylene blue staining of the prey *Voromonas pontica* and prey *Percolomonas cosmopolitus*. Panels A-C, biflagellate predator *V. pontica*. Black arrows indicate flagella of both protists (A-D). Panel D, tetraflagellate prey *P. cosmopolitus*. Black arrows in panel D indicate flagella of mature trophozoites of the prey and white arrows show juvenile trophozoite stages of the prey. The flagella of both predator and prey were detected; Panel E, the predator *V. pontica* (yellow arrow) and prey *P. cosmopolitus* (red arrow) attached in myzocytosis. The black arrow in panel E shows the tubular tether formed between predator and prey during myzocytosis and used to aspirate cytoplasmic contents of the prey. Cells from diprotist culture were formalin-fixed. Scale bars panels A-D, 20 μm; panel E, 30μm.

Yellowe's trichrome A (Figure 6C) and oocysts (red arrows) were detected. Giemsa staining routinely used for staining methanol-fixed smears of *P. falciparum* and *C. parvum* was also used in this study for comparison. Both *P. falciparum* and *C. parvum* stained with Giemsa stain (Figure 6 B and D, respectively) identified ring stages of *P. falciparum* (Figure 6B) and oocysts of *C. parvum* (Figure 6D).

In order to evaluate dyes obtained from different vendors for consistency and reproducibility in staining protocols, we used neutral red, brilliant green and methylene blue combinations from different vendors to stain *Colpodella* sp. ATCC 50594 (Table 1). Figure 7 A-C shows the type of variations in color obtained. Slight color variations were obtained when neutral red from different vendors was used. However, trophozoites and cyst stages of predator and prey were clearly identified (Figure 7 A-C).

Discussion

In previous studies, we developed staining protocols to aid routine light microscopic examination of *Colpodella* sp. ATCC 50594 and its prey *P. caudatus,* and to distinguish cysts of both protists in a diprotist culture [24]. Light microscope visualization of stained life cycle stages allowed for clearer interpretations of transmission electron micrographs, led to the identification of previously undocumented stages in the life cycle of *Colpodella* sp. ATCC 50594 and aided the description of the life cycle of *Colpodella* sp. ATCC 50594 in
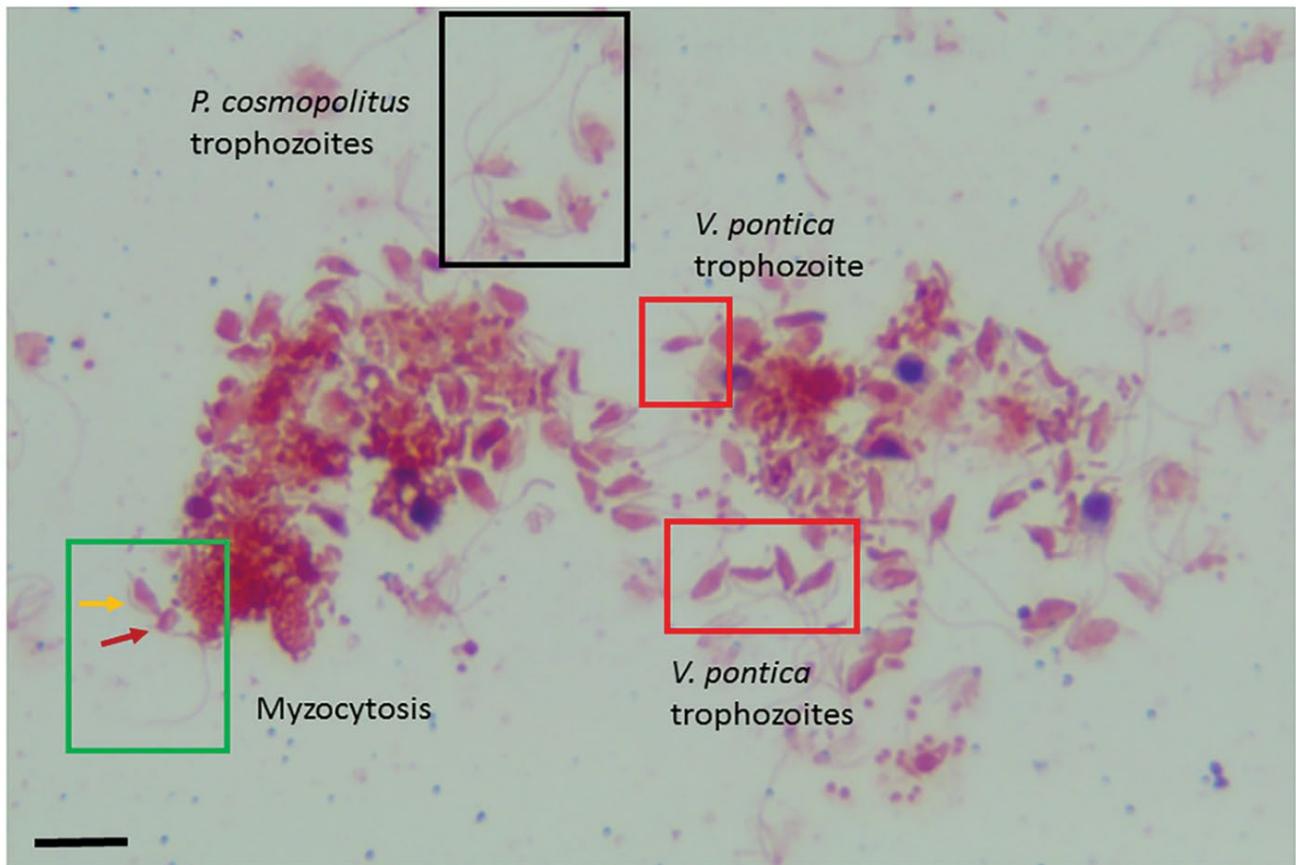
Figure 4: Sam-Yellowe's trichrome I staining of a diprotist culture of the marine predator *Voromonas pontica* (bi-flagellate) and its prey *Percolomonas cosmopolitus* (tetraflagellate). *Percolomonas cosmopolitus* trophozoites (black box), *V. pontica* (red box) and cells in myzocytosis (green box), *V. pontica* (yellow arrow) and *P. cosmopolitus* (red arrow) attached in the process of myzocytosis. Cells from diprotist culture were formalin-fixed. Scale bar, 20 μm.
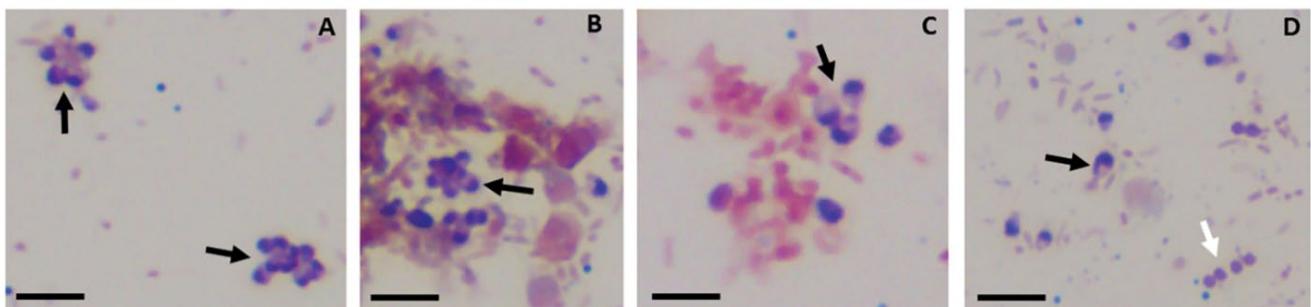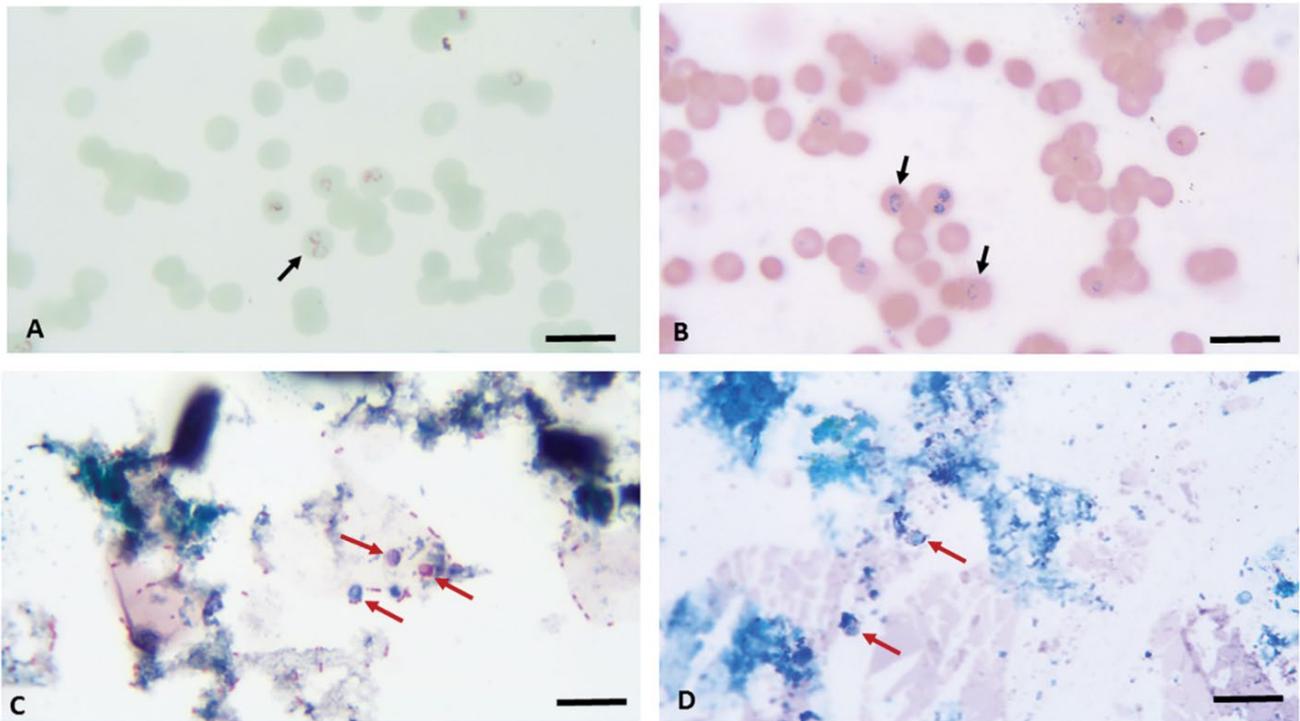

Figure 5: Sam-Yellowe's trichrome I staining of a diprotist culture of *Voromonas pontica* and *P. cosmopolitus* showing cyst stages of *V. pontica* (black arrows, panels A-D) and *P. cosmopolitus* (white arrow, panel D). Cysts of *V. pontica* were observed in groups (panels A-C) or observed individually (panel D black arrow). Cells from diprotist culture were formalin-fixed. Scale bars, 20 μm.

culture [23]. During myzocytosis, the trophozoite stage of *Colpodella* sp. ATCC 50594 forms a posterior food vacuole containing aspirated cytoplasmic contents from the prey. At the conclusion of feeding, a pre-cyst stage develops and the trophozoite differentiates into a cyst stage. Mitosis occurs within the cyst resulting in the development of juvenile trophozoites that emerge from the cyst following excystation [23]. Previous investigations of staining protocols for *Colpodella* sp. ATCC 50594 included the use of monochrome and dichrome staining protocols, using individual basic and acidic dyes or the use of dyes in combinations, and the use of commercial PROTO-FIX Trichrome stain (Wheatley's

modification) [24]. Poor differentiation of stages with these and more acidic dye combinations led to the development of the three-color dye protocols used in the present study [24]. The following dyes; Aqueous Fast green or Fast green in 0.5 % alcohol, Methyl green, malachite green and Janus green were substituted for brilliant green resulting in an overall reddish hue in the final color. However, life cycle stages were still identified regardless of the combination.

Two major goals of the current study were firstly, to demonstrate that dyes obtained from different vendors used in Sam-Yellowe's trichrome staining protocols could identify life cycle stages of *Colpodella* sp. ATCC 50594,

Figure 6: Sam-Yellowe's trichrome A and Giemsa staining of *Plasmodium falciparum* and *Cryptosporidium parvum*. Ring and trophozoite stages of methanol-fixed *P. falciparum* were stained by Sam-Yellowe's trichrome A (panel A) and Giemsa stain (panel B). Black arrows show ring stages of *P. falciparum*. Oocysts of *C. parvum* were stained with Sam-Yellowe's trichrome A (panel C) and Giemsa stain (panel D). Red arrows show oocysts of *C. parvum.* Scale bars, 20 μm.
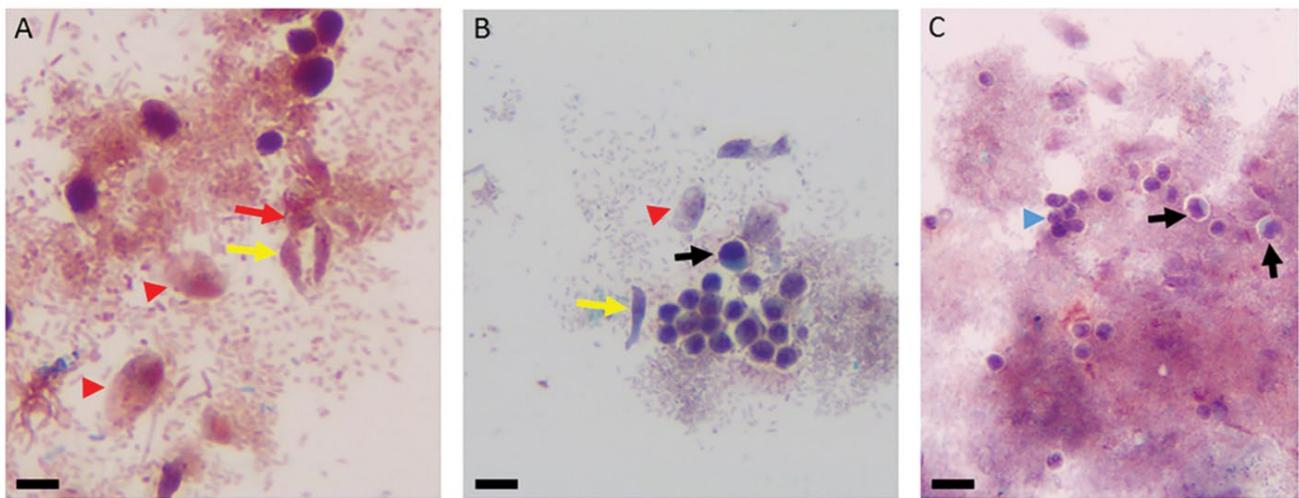
Figure 7: Sam-Yellowe's trichrome A performed using neutral red dye from three different major vendors. A, Carolina neutral red; B, ScholARs neutral red and C, Ward's (old) neutral red. Brilliant green from ACROS and methylene blue from EMD were used for the staining protocol. Panel A, yellow arrows indicate *Colpodella* sp. ATCC 50594 trophozoites attached in myzocytosis with its prey *Parabodo caudatus* (red arrow). Panel B, shows a young *Colpodella* sp. ATCC 50594 trophozoite (yellow arrow), *P. caudatus* trophozoite (red arrowhead) and a young demilune *Colpodella* sp. cyst (black arrow). Panel C shows young demilune *Colpodella* sp. ATCC 50594 cysts (black arrows) and *P. caudatus* cysts (blue arrowhead). Young demilune cysts of *Colpodella* sp. stain partially light blue-white and dark blue-purple compared to cysts of *P. caudatus* that are stained uniformly bluish-purple. 1% neutral red used in panel B was from the last lot purchased from ScholAR Chemistry before the company closed. Scale bars, 10 μm.

particularly young trophozoite and cyst stages. Secondly, we wanted to identify and distinguish cyst stages of *V. pontica* (formerly *Colpodella pontica*) and *P. cosmopolitus* using Sam-Yellowe's trichrome staining series. Cyst stages of *V. pontica* and *P. cosmopolitus* have not been described using light microscopy. In the last decade, human and animal infections by novel strains of *Colpodella* species have been reported and

increased reports of the detection of *Colpodella* sp. in ticks, biting flies and pet dogs and cats have been made [11,19,26-28]. Furthermore, *Colpodella* sp. have been identified in ticks during surveillance studies to identify the presence and distribution of pathogens in the ticks [26,27]. The identification of *Colpodella* sp. in ticks and the association of tick bites in animal and human infection suggests the potential

for zoonotic infections with ticks transmitting *Colpodella* sp. from animals to humans [11,19]. In the reported human and animal cases, molecular techniques using PCR and DNA sequencing identified sequences homologous to strains and species of *Colpodella* sp. identified in human infections [10,11]. DNA obtained from animal specimens, ticks and soil were also found to be homologous to the strains identified in human infections [18,19,26,27]. However, in all the cases reported, the life cycle stages of *Colpodella* sp. transmitting infection or responsible for pathogenesis was not described [11,12,18,19,26-28], and the mechanism of infection is unknown. The staining protocols described in this study can aid morphological identification of life cycle stages in human and animal specimens. Bi-flagellated trophozoites of *Colpodella* sp. can be identified as fusiform shaped cells. Immature and mature cysts can be identified as irregularly shaped spheres, with the characteristic demilune colors of the young cyst stage [24]. Both stages are easily identified and distinguished from the life cycle stages of the prey and in the background of bacteria present in the culture. If attachment of *Colpodella* sp. to human and animal cells occurs during infection, the staining protocols will identify such attachments. In previous studies from our lab, we have used Sam-Yellowe's trichrome staining to identify and characterize predator and prey attached in myzocytosis [8,23]. Knowledge of transmission and pathogenic stages of *Colpodella* will aid proper diagnosis of infections caused by *Colpodella* species and avoid the confusion of infections caused by *Colpodella* sp. with *Babesia* sp. or *Plasmodium* sp. Yuan et al. and Neculicioiu et al. reported the use of Giemsa staining to identify *Colpodella* sp. [10,12]. However, details of the life cycle stages observed were not described. The search for accessible and rapid staining protocols to identify life cycle stages of pathogens and to aid diagnosis is an area of intense investigations as reported for cyst stage detection in *Acanthamoeba* sp. [29]. The number of tick species harboring *Colpodella* species continues to increase with recent reports in the tick *Hyalomma domedarii* infesting camels in Egypt and *Rhipicephalus bursa* infesting cattle in Italy [30,31]. We show for the first time that the cysts of *V. pontica* and *P. cosmopolitus* in culture can be distinguished. Routine light microscopy to identify colpodellids can be achieved with specimen staining in less than ten minutes using Sam-Yellowe's trichrome stains. Distinct features of *V. pontica* morphology including the heterodynamic flagella and cell shape can be identified with the use of Sam-Yellowe's trichrome stains. Due to the identification of *Colpodella* sp. in diverse geographic locations and the confusion of symptoms in the reported cases with symptoms of babesiosis and malaria, we wanted to demonstrate that the staining protocol is robust enough to clearly differentiate other protists if present, in different tissue specimens from hosts in different geographic environments [10,11,19,26]. In this study we show that Sam-Yellowe's trichrome staining protocols developed to identify trophozoite and cyst stages of *Colpodella* sp. ATCC 50594 can be used to identify life cycle stages of the pathogenic apicomplexans *P. falciparum* and *C. parvum*. *Plasmodium falciparum* ring-infected erythrocytes in the blood stage and oocysts, of *C. parvum* were identified by the staining protocols [24]. The oocysts were easily recognized with Sam-Yellowe's trichrome staining when compared to Giemsa staining. In mixed infections of piroplasms and *Colpodella* sp. in blood, life cycle stages of each protist can be distinguished. Similarly, in mixed *Cryptosporidium* sp. and *Colpodella* infections, protists can be identified in fecal samples, and specific life cycle stages identified. Sam-Yellowe's trichrome staining protocol is completed in less than 10 minutes resulting in vibrant colors that clearly distinguish life cycle stages providing good contrast and differentiation of developmental stages of trophozoites and cysts in the colpodellids [24]. We show that dyes obtained from different vendors produce minor color variations in stained cells without affecting the identification of life cycle stages of *Colpodella* sp. ATCC 50594. The use of the staining protocol to identify new *Colpodella* species will provide a clearer understanding of morphological similarities and differences among *Colpodella* species. Since neutral red can no longer be purchased from ScholAR Chemistry, we have evaluated neutral red from different vendors and find consistent and reproducible final colors using EMS neutral red. In this study, we report for the first time the identification of the cyst stages of *V. pontica* by light microscopy and demonstrate that Sam-Yellowe's trichrome staining protocols are robust enough to identify *Colpodella* sp. trophozoite and cyst stages in human and animal specimens, in ticks, flies and environmental samples such as in soil and water.

Author Contributions

Conceptualization, T.S.Y.; methodology, M.S; O.E.A; software, T.S.Y.; validation, T.S.Y, M.S., and O.E.A., ; formal analysis, T.S.Y., M.S., and O.E.A..; investigation, T.S.Y., M.S., and O.E.A.; resources, T.S.Y.; data curation, T.S.Y.; writing—original draft preparation, T.S.Y, M.S., and O.E.A.; writing—review and editing, T.S.Y.; visualization, T.S.Y., M.S., and O.E.A.; supervision, T.S.Y..; project administration, T.S.Y.; funding acquisition, T.S.Y.

Acknowledgments

Funding information

Conflicts of Interest

On behalf of all authors, the corresponding author states that there is no conflict of interest.

References

1. Kuvardina ON, Leander BS, Aleshin VV, Myl'nikov AP, Keeling PJ, et al. (2002) The phylogeny of colpodellids (Alveolata) using small subunit rRNA gene sequences suggests they are the free-living sister group to apicomplexans. J Eukaryot Microbiol 49: 498-504.

2. Gile GH, Slamovits CH (2014) Transcriptomic analysis reveals evidence for a cryptic plastid in the colpodellid *Voromonas pontica*, a close relative of chromerids and apicomplexan parasites. PLoS One 9: e96258.

3. Olmo JL, Esteban GF, Finlay BJ (2011) New records of the ectoparasitic flagellate *Colpodella gonderi* on non-*Colpoda* ciliates. J Int Microbiol 14: 207-211.

4. Cavalier-Smith T, Chao EE (2004) Protalveolate phylogeny and systematics and the origins of Sporozoa and dinoflagellates (phylum Myzozoa nom. Nov.). Eur J Protistol 40: 185-212.

5. Simpson AGB; Patterson DJ (1996) Ultrastructure and identification of the predatory flagellate *Colpodella pugnax* Cienkowski (Apicomplexa) with a description of *Colpodella turpis* n. sp. and a review of the genus. Syst Parasitol 33: 187-198.

6. Brugerolle G (2002) *Colpodella vorax*: Ultrastructure, predation, life-cycle, mitosis, and phylogenetic relationships. Europ J Protistol 38: 113-125.

7. Mylnikov AP, Mylnikova ZM (2008) Feeding spectra and pseudoconoid structure in predatory alveolate flagellates. Inland Water Biol 1: 210-216.

8. Sam-Yellowe TY, Fujioka H, Peterson JW (2022) Ultrastructure of Myzocytosis and Cyst Formation, and the Role of Actin in Tubular Tether Formation in *Colpodella* sp. (ATCC 50594). Pathogens 11: 455.

9. Mylnikov AP (2009) Ultrastructure and phylogeny of colpodellids (Colpodellida, Alveolata). Biol Bulletin 36:582-590.

10. Yuan CL, Keeling PJ, Krause PJ (2012) *Colpodella* spp.–like Parasite Infection in Woman, China. Emerg Infect Dis 18: 125-127.

11. Jiang JF, Jiang RR, Chang QC, Zheng YC, Jiang BG, et al. (2018) Potential novel tick-borne *Colpodella* species parasite infection in patient with neurological symptoms. PLOS Negl Trop Dis 12: e0006546.

12. Neculicioiu VS, Colosi IA, oc DA, Lesan A, Costache C (2021) When a ciliate meets a flagellate: A rare case of *Colpoda* spp. and *Colpodella* spp. isolated from the urine of a human patient. Case report and brief review of the literature. Biology (Basel) 10: 476.

13. Squarre D, Nakamura Y, Hayashida K, Kawai N, Chambaro H, et al. (2020) Investigation of the piroplasm diversity circulating in wildlife and cattle of the greater Kafue ecosystem, Zambia. Parasit Vectors 13: 599.

14. Solarz W, Najberek K, Wilk-Wozniak E, Biedrzycka A (2020) Raccoons foster the spread of freshwater and terrestrial microorganisms-mammals as source of microbial eDNA. Divers Distrib 26: 453-459.

15. Wheatley MA, Shamoun J, Maggi R, Breitschwerdt EB, Sommer SL, et al. (2023) Eosinophilic pericardial effusion and pericarditis in a cat. JFMS Open Rep 9: 20551169231213498.

16. Huggins LG, Colella V, Koehler AV, Schunack B, Traub RJ (2022) A multipronged next-generation sequencing metabarcoding approach unearths hyperdiverse and abundant dog pathogen communities in Cambodia. Transbound Emerg Dis 69: 1933-1950.

17. Qi Y, Wang J, Lu N, Qi X, Yang C, et al. (2024) Potential novel *Colpodella* spp. (phylum Apicomplexa) and high prevalence of *Colpodella* spp. in goat-attached *Haemaphysalis longicornis* ticks in Shandong province, China. Ticks Tick Borne Dis 15: 102328.

18. Xu M, Hu Y, Qiu H, Wang J, Jiang J (2022) *Colpodella* sp. (Phylum Apicomplexa) Identified in Horses Shed Light on Its Potential Transmission and Zoonotic Pathogenicity. Front Microbiol 13: 857752.

19. Chiu HC, Sun X, Bao Y, Fu W, Lin K, et al. (2022) Molecular identification of *Colpodella* sp. of South China tiger *Panthera tigris amoyensis* (Hilzheimer) in the Meihua Mountains, Fujian, China. Folia Parasitol (Praha) 69: 2022.019.

20. Hussein S, Li X, Bukharr SM, Zhou M, Ahmad S, et al. (2021) Cross-genera amplification and identification of *Colpodella* sp. with *Cryptosporidium* primers in fecal samples of zoo felids from northeast China. Braz J Biol 83: e247181.

21. Neupane S, Saski C, Nayduch D (2021) House fly larval grazing alters dairy cattle manure microbial communities. BMC Microbiol 21: 346.

22. Phetkarl T, Fungwithaya P, Udompornprasith S, Amendt J, Sontigun N (2023) Preliminary study on prevalence of hemoprotozoan parasites harbored by *Stomoxys* (Diptera: Muscidae) and tabanid flies (Diptera: Tabanidae) in horse farms in Nakhon Si Thammarat province, Southern Thailand. Vet World 16: 2128-2134.

23. Getty TA, Peterson JW, Fujioka H, Walsh AM, Sam-Yellowe TY (2021) *Colpodella* sp. (ATCC 50594) Life Cycle: Myzocytosis and Possible Links to the Origin of Intracellular Parasitism. Trop Med Infect Dis 6: 127.

24. Sam-Yellowe TY, Addepalli K, Yadavalli R, Peterson JW (2019) New trichrome stains identify cysts of *Colpodella* sp. (Apicomplexa) and *Bodo caudatus*. J Int Microbiol 23: 303-311.

25. Sam-Yellowe TY, Yadavalli R (2019) *Voromonas pontica* Identified by Giemsa Staining and Anti-RhopH3 Protein Reactivity. J Microbiol Modern Tech 4: 103.

26. Matsimbe AM, Magaia V, Sanchez GS, Neves L, Noormahomed E, et al. (2017) Molecular detection of pathogens in ticks infesting cattle in Nampula province, Mozambique. Exp Appl Acarol 73: 91-102.

27. Zhao GP, Wang YX, Fan ZW, Ji Y, Liu MJ, et al. (2021) Mapping ticks and tick-borne pathogens in China. Nat Commun 12: 1075.

28. Wu S, Meng J, Yu F, Zhou C, Yang B, et al. (2023) Molecular epidemiological investigation of piroplasms carried by pet cats and dogs in an animal hospital in Guiyang, China. Front Microbiol 14: 1266583.

29. El-Sayed NM, Hikal WM (2015) Several staining techniques to enhance the visibility of *Acanthamoeba* cysts. Parasitol Res 114: 823-830.

30. Soliman AM, Mahmoud HYAH, Hifumi T, Tanaka T (2024) Discovery of *Colpodella* spp. in ticks (*Hyalomma domedarii*) infecting camels in southern Egypt. Ticks and Tick-borne Diseases 5: 102352.

31. Jimale KA, Bezerra-Santos MA, Mendoza-Roldan JA, Latrofe MS, Baneth G, et al. (2024) Molecular detection of *Colpodella* sp. and other tick-borne pathogens in ticks of ruminants, Italy. Acta Tropica 257: 107306.